ACS OMEGA

http://pubs.acs.org/journal/acsodf

Article

Coal Wall and Roof Segmentation in the Coal Mine Working Face Based on Dynamic Graph Convolution Neural Networks

Zhizhong Xing, Shuanfeng Zhao,* Wei Guo, Xiaojun Guo, Shenquan Wang, Junjie Ma, and Haitao He

Cite This: *ACS Omega* 2021, 6, 31699−31715

Read Online

ACCESS | Metrics & More | Article Recommendations

ABSTRACT: The intersection line information of the point cloud between the coal wall and the roof can not only accurately reflect the direction information of the scraper conveyor but also provide a preliminary basis for realizing the intelligent coal mine. However, the indirect method of using deep learning to segment the point cloud of coal mine working face cannot make full use of the rich information provided by the point cloud data. The direct method of using deep learning to segment the point cloud ignores the local feature relationship between points. Therefore, we propose to use dynamic graph convolution neural networks (DGCNNs) to segment the point cloud of the coal wall and roof so as to obtain the intersection line between them. First, in view of the characteristics of heavy dust and strong electromagnetic interference in the environment of the coal mine working face, we have installed an underground inspection robot so that we use light detection and ranging to obtain the point cloud of the coal mine working face. At the same time, we put forward a fast labeling method of the point cloud of the coal mine working face and an efficient training method of the depth neural network. Second, on the basis of edge convolution, being the greatest innovation of DGCNNs, we analyze the influence of the number of layers, *K* value, and output feature dimension of edge convolution on the effect of DGCNNs segmenting the point cloud of the coal mine working face and obtaining the intersection line of the coal wall and roof. Finally, we compare DGCNNs with PointNet and PointNet++. The results show that the DGCNN exhibits the best performance. What is more, the results provide a research foundation for the application of DGCNNs in the field of energy. Last but not least, the research results provide a direct and key basis for the adjustment of the scraper conveyor, which is of great significance for an intelligent coal mine working face and accurate construction of a geological information model.

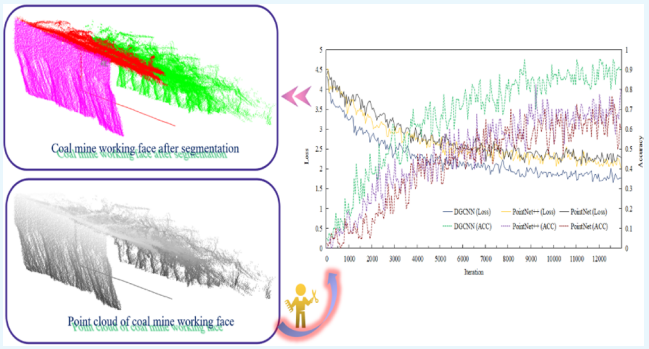

1. INTRODUCTION

Coal is a combustible solid that is formed through complex chemical and physical reactions.[1] As the core technical support for safe and efficient production of the coal mine, the intelligent coal mine is an important direction for the development of fossil fuel-related fields.[2−4] Due to the complexity and limitations of the underground environment and the influence of coal dust and water mist, as well as electromagnetic interference in the workplace, the accurate acquisition of the direction information of the scraper conveyor has become an urgent problem to be solved, which can realize the intelligent coal mine working face.[5−7]

A scraper conveyor not only loads and transports falling coal but also is the track of a shearer. The existing research generally obtains the direction information of the scraper conveyor by detecting the position of the shearer. Among them, in the research of inertial navigation technology, Einicke et al.[8] used inertial elements to locate the shearer, studied the positioning error compensation technology, and proposed the shearer positioning method based on the minimum variance smoothing filter. In the research of the combined positioning method, Yang et al.[9] studied the error compensation method of a strapdown inertial navigation system. By establishing the error compensation model, the accumulated error of sensors on the shearer is reduced and the detection accuracy of the inertial navigation system is improved. Fan et al.[10] used a strapdown gyroscope as the main positioning system and used wireless sensor networks to align the strapdown gyroscope regularly so as to eliminate the accumulated error of inertial elements working for a long time. However, the above-mentioned methods have their own defects. The vibration of the shearer will greatly reduce the sensing accuracy of the

Received: August 14, 2021
Accepted: November 4, 2021
Published: November 15, 2021

gyroscope. The way of obtaining the positioning of the shearer through an inertial navigation system will cause large cumulative errors. What is more, the combined positioning method still cannot avoid the inherent defects of inertial navigation. The correction error will directly affect the accuracy of the inertial navigation system. If the correction system is disturbed, the combined positioning accuracy will be seriously affected.[11] Most importantly, to realize the positioning of the shearer in the whole working face, we not only need inertial navigation sensors with higher accuracy, increasing the technical cost, but also need to study the combined positioning method with high accuracy and low cost.

Lasers have the characteristics of good unidirectionality and strong anti-interference ability. Compared with visible light, the laser has stronger dust fog penetration ability. Also, the laser point cloud can more accurately reflect the spatial relationship of various parts in the coal mine working face.[12−15] In addition, the intersection line of the coal wall and roof can reflect the cutting track of the shearer and the direction information of the scraper conveyor. Therefore, we segment the laser point cloud of the coal wall and roof through the spatial feature of point cloud data, so as to obtain their intersection line information, which can provide a key basis for the straightening and inclining of the scraper conveyor. This research can provide the premise and direct data basis for building an accurate geological information model of the coal mine working face. Most importantly, it is of great significance for the realization of an intelligent and unmanned coal mine working face.

At present, the field of the point cloud segmentation algorithm has been developed and improved. According to different segmentation principles, there are three traditional methods of point cloud segmentation.[16−18] The first one is the point cloud segmentation algorithm based on the boundary. In principle, the segmentation method based on the boundary is to detect the boundary between regions in the point cloud, so as to find the points whose geometric features (such as normal vector or curvature) change quickly, and then to complete the segmentation of the point cloud. In the research of this aspect, Woo et al.[19] divided the point cloud through the spatial grid and used the normal vector deviation as the basis for further subdivision of the point cloud grid to realize the point cloud segmentation. The other is the point cloud segmentation algorithm based on model fitting. This method mainly parameterizes the structural elements of objects (such as plane, surface, cylinder, etc.) in the point cloud so as to realize the point cloud segmentation by the model equation. Limberger and Oliveira[20] extended the classic kernel-based hough transform (KHT) to 3D space so as to realize the point cloud segmentation in the point cloud with irregular distribution and noise. The last one is the point cloud segmentation method based on clustering. The method regards the points with certain geometric parameters as clusters. Sampath and Shan[21] first calculated the probability that each point in the point cloud can be used as the clustering center and then used fuzzy k-means to realize the point cloud segmentation. Yang et al.[22] designed an improved breadth first search algorithm to update the clustering of point clouds so as to realize the segmentation of point clouds.

However, the segmentation method based on boundary often requires a large amount of computation, and it is easily affected by the environmental noise; therefore, the segmentation effect of scattered and irregular point clouds is not ideal.[23,24] In addition, the disadvantage of the segmentation method based on model fitting is that the threshold is usually fixed in the process of model parameter calculation, and its segmentation accuracy and efficiency are affected by the point cloud source to a certain extent, so it cannot adapt to the segmentation of complex point cloud environment with multiple geometric types.[25,26] The disadvantage of point cloud segmentation based on clustering is that the clustering criteria are not unified. Different clustering methods are often only suitable for specific types of point clouds, and the portability of these methods is poor. What is more, the results of point cloud segmentation based on clustering are often prone to small-scale point cloud clustering, which needs post-processing (such as clustering merging).[27]

In recent years, with the extensive application of deep learning in computer vision, image processing, and other fields, deep learning has been greatly developed.[28−32] The deep learning methods of point cloud segmentation are mainly divided into indirect methods and direct methods. As point cloud is a kind of unstructured data distributed in 3D space, it is quite different from image data in organization and expression. Therefore, when the deep neural network (DNN) is applied to the point cloud segmentation, it is necessary to change the modality of the point cloud, and then, we use different DNNs to get the corresponding results.[33−35] In the process of transforming the point cloud into a 2D image, Lawin et al.[36] transformed the input point cloud into view images such as depth and color through projection and then sent these generated view images to convolution neural networks (CNNs) to realize the segmentation of the point cloud. Wang et al.[37] rendered 3D point clouds from different perspectives to get 2D images and realized the segmentation of point clouds by using multiview CNNs (MVCNNs). Zhao et al.[38] transformed the point cloud into a multiscale feature map, then used the CNN to segment the point cloud, and optimized the research results by using the traditional machine learning method. In the process of transforming the point cloud into 3D voxels, Zhou and Tuzel[39] divided the point cloud into equidistant 3D voxels, introduced the voxel feature coding layer in VoxelNet, and transformed a group of points in each voxel into unified features for segmentation. Wu et al.[40] expressed the point cloud as the probability distribution of binary variables on the 3D voxel grid through ShapeNets and used the convolution depth confidence network to process the point cloud. Graham et al.[41] proposed sparse convolution operation and constructed sparse convolution networks to segment point clouds in voxels. The network pays more attention to the occupied voxels, reduces unnecessary calculation, and achieves better segmentation results. Qi et al.[42] of Stanford University creatively proposed a deep learning network structure PointNet, which can directly process point cloud data, breaking the bottleneck in the field of point cloud research and playing a pioneering role in the development of deep learning in the field of point cloud data. PointNet directly uses the original point cloud as input, which need not convert the point cloud to other formats and uses a symmetric function to solve the disorder problem of the point cloud. In the process of segmentation, PointNet uses the shared multilayer perceptron to replace the convolution operator and finally gets the classification probability of each point so as to complete the segmentation of the input point cloud.

However, in the indirect method, the depth learning method based on 2D projection will lose part of the spatial information

https://doi.org/10.1021/acsomega.1c04393
ACS Omega 2021, 6, 31699−31715

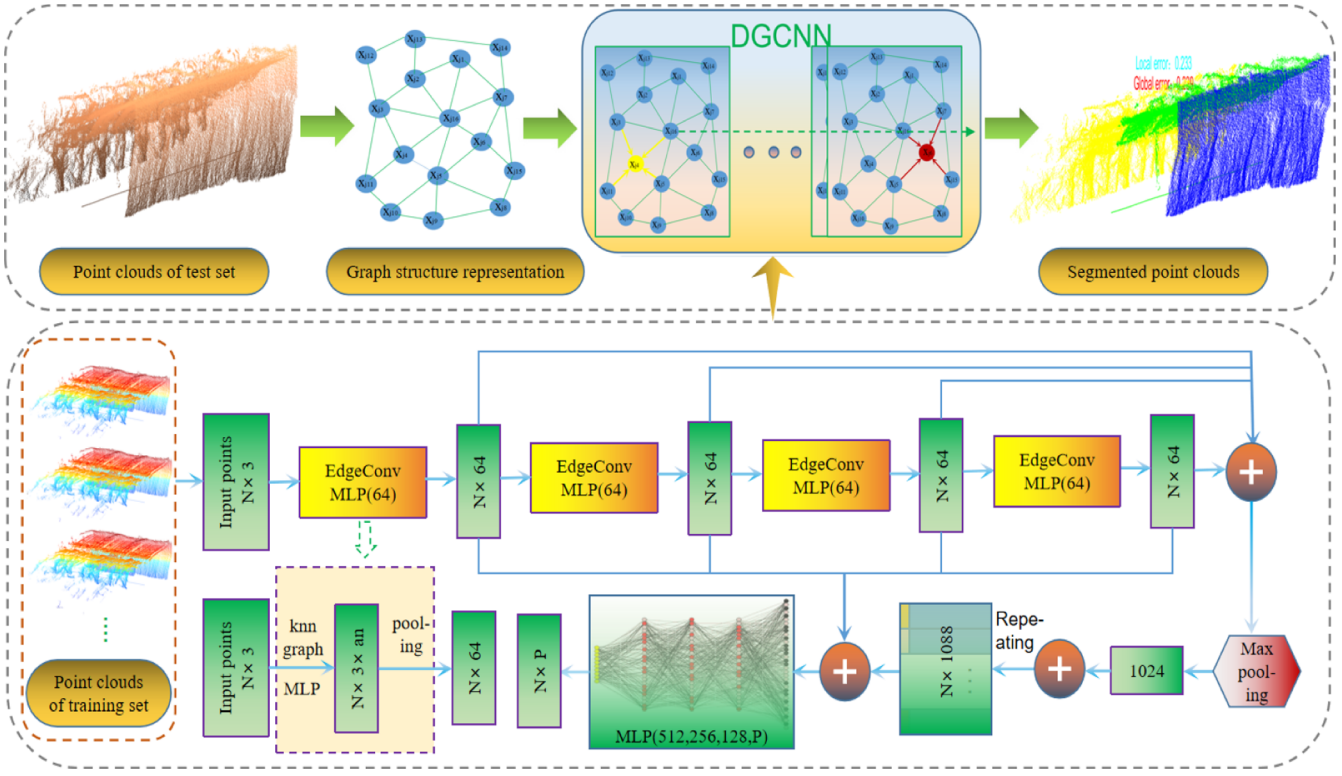

Figure 1. Point cloud segmentation of the coal mine working face by the DGCNN (top) and to learn the features of the point cloud of the coal mine working face by the DGCNN (bottom).

in the process of point cloud projection, resulting in the loss of point cloud data information, which affects the final segmentation accuracy.[43] The disadvantage of point cloud segmentation based on the voxelization method is that it is difficult to extract the fine-grained features of point cloud data; therefore, this method cannot make full use of the rich information provided by point cloud data.[44] Although PointNet has a pioneering achievement in the process of directly extracting point cloud features from point cloud data for segmentation, it does not consider the local neighborhood information of point cloud data. The feature extraction process of PointNet on each point of the point cloud only considers the global features in the point cloud data and ignores the local feature relationship between points.[45] Dynamic graph convolution neural networks (DGCNNs) are new DNNs for processing point clouds. For each point in the point cloud data, the DGCNN not only considers the features of the current point but also considers the features of k points nearest to the center point in the current feature space, which takes into account the relationship between the point and the adjacent edge, so that local neighborhood features can be extracted from the local graph composed of k points.[46] The DGCNN takes into account both global and local features and considers the relationship between points, which greatly reduces the loss of effective information of the target. It has a broad application prospect in point cloud processing in energy engineering, bioengineering, and other fields.[47] Therefore, we put forward the DGCNN as a DNN to segment the point cloud of the coal mine working face and deeply analyze and improve its network architecture so as to make the DGCNN better learn the feature information of the point cloud of the coal mine working face and obtain better results.

Most importantly, the application of DGCNNs in point cloud segmentation of the coal mine working face is still blank. At the same time, the research team of the author has installed a special track to run the inspection robot outside the scraper conveyor and has obtained the point cloud of the coal mine working face by using the light detection and ranging (LiDAR) on the inspection robot. According to the author's previous research results, the markers in the coal mine working face can be found through DGCNNs, and then, the point cloud coordinate of the coal mine working face can be converted to the geodetic coordinate system.[48] However, further research still needs to be carried out. Whether DGCNNs can segment the coal wall and the roof and accurately obtain the intersection line of the coal wall and roof has not been known, and whether DGCNNs can achieve a good application effect in the field of energy and geology has also not been known. Therefore, we propose to use DGCNNs to process the point cloud of the coal mine working face so that the depth neural network can better learn the local and global features of the point cloud of the coal mine working face and fit the point cloud of the coal wall and roof after segmentation, so as to obtain the intersection line information of the two, which provides a direct data basis for the straightening and inclining adjustment of the scraper conveyor, provides a premise for the intelligent height adjustment of the shearer, and makes a beneficial exploration for the realization of intelligent and unmanned mining. At the same time, it provides a new method to obtain the intersection line of coal wall and roof in coal mine working face.

The rest of this paper is organized as follows: Section 2 introduces the details of our proposed DGCNN, as well as the materials and methods of making data sets. Section 3 describes

https://doi.org/10.1021/acsomega.1c04393
ACS Omega 2021, 6, 31699−31715

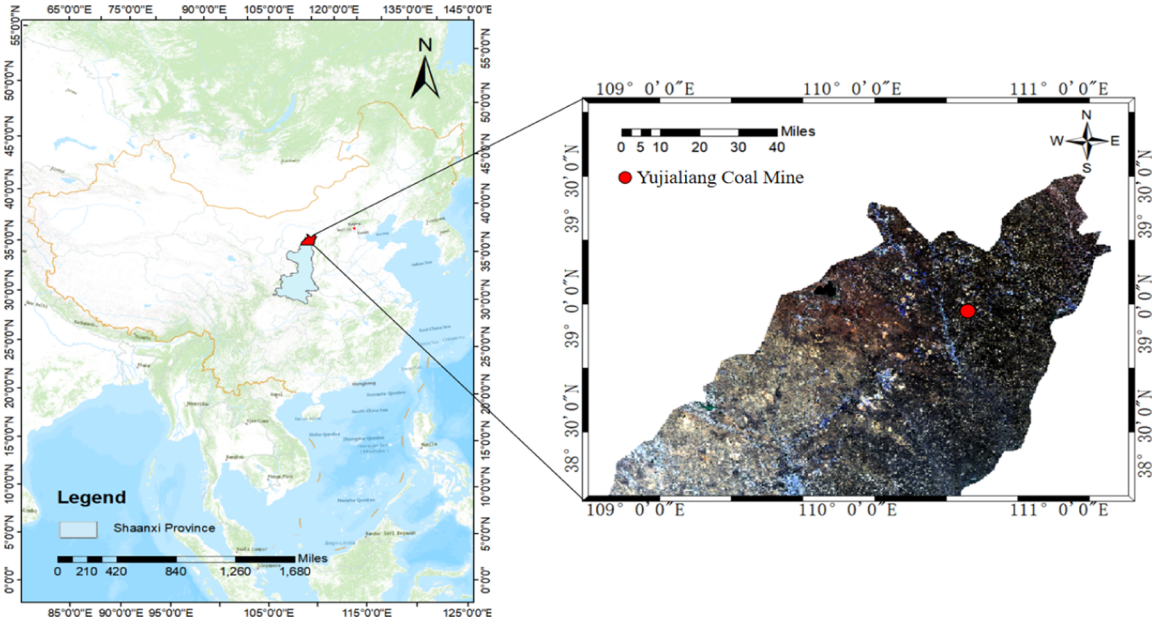

Figure 2. Location of the study site.

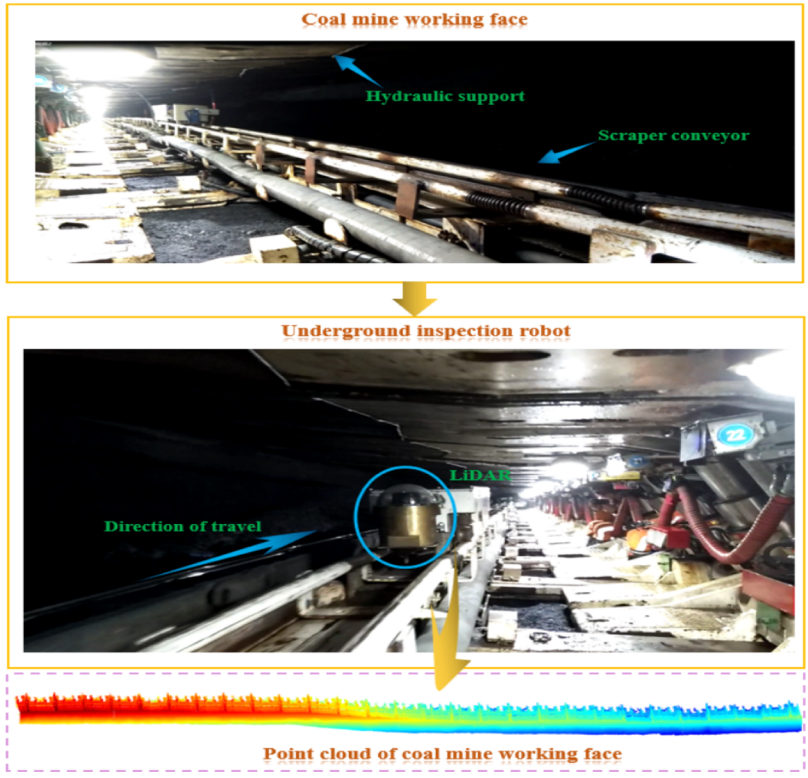

Figure 3. Coal mine working face in Yujialiang coal mine (top) and the underground inspection robot in the coal mine working face (middle) and the point cloud of the coal mine working face collected by LiDAR (bottom).

the experiments and result analysis. The conclusions and further work are detailed in the last sections.

2. MATERIALS AND METHODS

At present, in intelligent mining, the segmentation method of the point cloud by the deep learning method is blank. In addition, the indirect method of using deep learning to deal with the point cloud of the coal mine working face will lose part of the spatial information of the point cloud and cannot make full use of the rich information provided by the point cloud data. However, the direct method of using deep learning to deal with the point cloud of the coal mine working face ignores the local feature relationship between points. We propose to use DGCNNs to learn the feature of the point cloud to segment the point cloud of the coal mine working face (Figure 1), so as to obtain the intersection line of the coal wall and roof, which provides the key basis for the straightening and

https://doi.org/10.1021/acsomega.1c04393
ACS Omega 2021, 6, 31699−31715

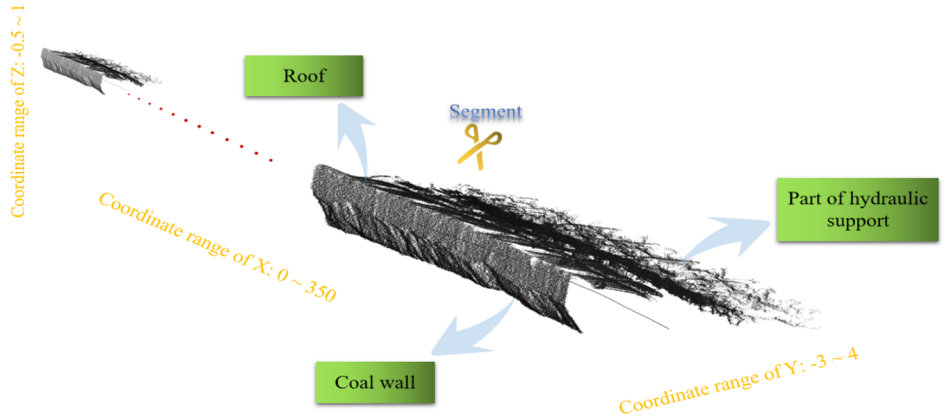

Figure 4. Coordinate range and marking method of the point cloud of the whole coal mine working face.

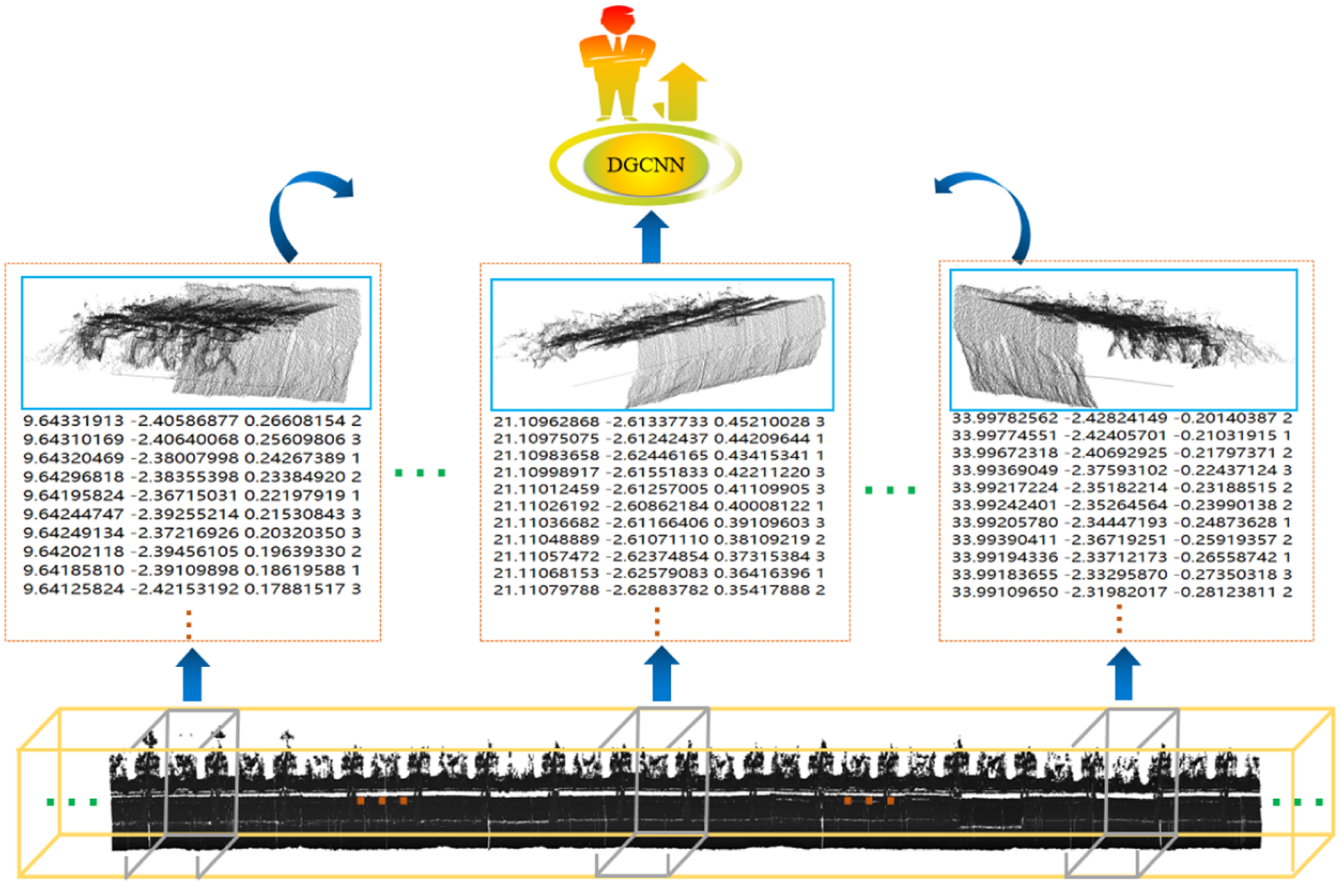

Figure 5. Point cloud training depth neural network in the coal mine working face.

inclining adjustment of the scraper conveyor. It also provides a premise for the realization of unmanned mining.

2.1. Materials and Methods of Making Data Sets. The research team of the author has installed an expensive underground inspection robot in Yujialiang mine in Yulin City, Shaanxi Province, China (Figure 2). The point cloud of the coal mine working face is collected by LiDAR on the underground inspection robot, as shown in Figure 3. Because the length of the whole coal mine working face is too long, in order to facilitate observation, we selected part of the coal mine working face point cloud for visualization.

Figure 3 shows that LiDAR runs along the special track outside the scraper conveyor in the coal wall extension direction so as to collect the point cloud of the whole coal mine working face. We use the "segment" function of Cloud Compare software to batch label the point cloud of the coal mine working face. The corresponding coordinate range and labeling method of the point cloud of the whole coal mine working face are shown in Figure 4.

We randomly select a section of the point cloud of the coal mine working face within the range of 0−300 m of the x-axis, so as to realize the training of different depth neural network models, and let the depth neural network fully learn the features of the point cloud of the coal mine working face, as shown in Figure 5. At the same time, we take the remaining 50

https://doi.org/10.1021/acsomega.1c04393
ACS Omega 2021, 6, 31699−31715

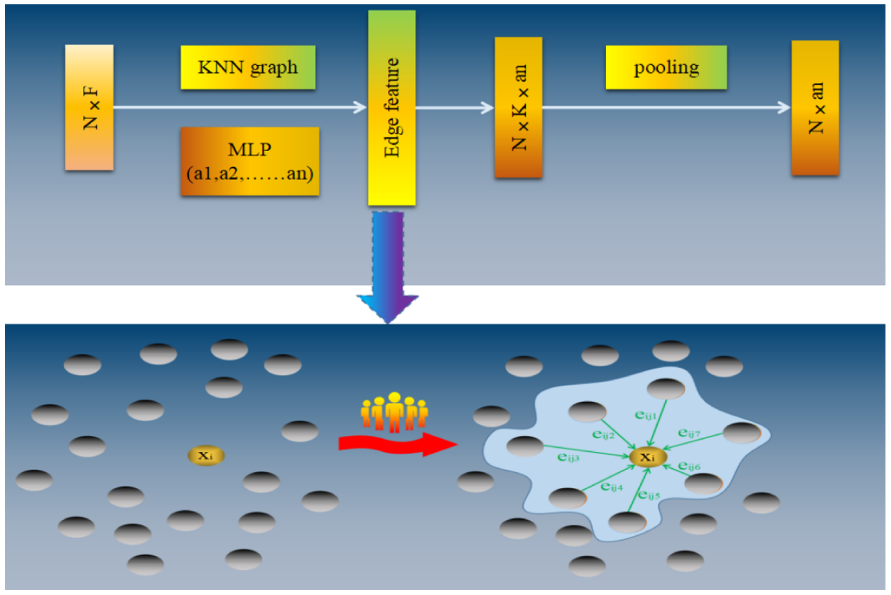

Figure 6. Structure of edge convolution (top) and edge convolution aggregate features of edges (bottom).

m of the point cloud in the coal mine working face as the test set.

As shown in Figure 5, we randomly select a section of the point cloud within 0−300 m of the coal mine working face to train the neural network. The first three digits of each point in each section of the point cloud are the 3D coordinates of the point, and the last digit represents the category label of the point. We use the abovementioned method not only to realize the fast labeling of the point cloud of the coal mine working face but also to realize the efficient and simple training of the DNN model without actually dividing the point cloud of the coal mine working face into multiple training data.

2.2. Edge Convolution Method in DGCNNs. In this study, a directed graph is used to represent the structure of the point cloud in the coal mine working face,[49,50] as shown in eq 1

$$G = (\nu,\ \varepsilon) \tag{1}$$

In eq 1, ν is the vertex, $\nu = [\nu_1, \nu_2, \ldots\ldots\nu_n]^T$ and $\varepsilon$is the edge, $\varepsilon \in \nu \times \nu$. According to the local graph structure of the center point x_i, we can find that the nearest point to the point $x_i$isx_{ji1},⋯, x_{jik}, and the adjacent points correspond to the directed edges(i, j_{i1}),⋯, (i, j_{ik}), respectively. The features of these edges can be expressed as eq 2.

$$e_{ij} = h_\Theta(x_i,\ x_j - x_i) = \mathrm{ReLU}[\beta\cdot(x_j - x_i) + \xi\cdot x_i] \tag{2}$$

where $h_\Theta(\cdot)$ is the edge feature extraction function, Θ is the hyperparameter to be learned by $h_\Theta(\cdot)$, $\Theta = (\beta_1,\ldots, \beta_i, \xi_1, \ldots, \xi_i)$, and i is the number of output channels. In DGCNNs, the input of the first level edge convolution layer is the point cloud X^0, and the output of the L layer edge convolution layer can be expressed as eq 3

$$X^{\mathrm{L}} = \{x_1^{\mathrm{L}}, \ldots,\ x_n^{\mathrm{L}}\} \subseteq R^{\mathrm{FL}} \tag{3}$$

where N is the number of points in the point cloud, R is the feature space, and F is the dimensional feature information of points. The edge features around the center point of the L layer in the DGCNN are determined by the k nearest neighbor points x_{ji1}, ⋯, x_{jik} around the center point, and the update of the center point of the L+1 layer can be expressed as eq 4

$$x_i^{\mathrm{L}+1} = \max_{j:(i,\ j)\in\Omega} h_\theta{}^{\mathrm{L}}(x_i^{\mathrm{L}},\ x_j^{\mathrm{L}}) \tag{4}$$

where max represents the maximum pooling operation and Ω is the receptive field area composed of the center point and the adjacent points. In practice, edge convolution computes the features of all the associated edges and the features of each vertex to obtain the high-dimensional features of the current graph structure. The overall framework of edge convolution in the DGCNN is shown in Figure 6.

As shown in Figure 6, the edge convolution module contains local neighborhood information, and it can obtain global information by stacking, that is, each center point can potentially represent a very long distance in the feature space. However, when the number of edge convolution layers reaches a certain number, each point will be too smooth so that the feature differentiation of each point is not obvious, which will affect the segmentation effect of the depth neural network on the point cloud. Therefore, we study the point cloud segmentation effect of edge convolution with different layers in Section 3.3.

2.3. K-Nearest Neighbor Graph Algorithm in Edge Convolution. The receptive field of conventional convolution will affect the effect of the DNN. The K-nearest neighbor (KNN) graph algorithm provides the range of the receptive field for edge convolution in DGCNNs, and the K value in the KNN graph algorithm will also affect the effect of the point cloud processing in DGCNNs.[51] In the KNN graph algorithm, in order to compare the differences between training samples and test samples, the Euclidean distance is selected for comparison, such as eq 5

$$\mathrm{dist}(X_1,\ X_2) = \sqrt{\sum_{i=1}^{m}(x_{i2} - x_{i1})^2} \tag{5}$$

where X_1 and X_2 represent two compared samples by the Euclidean distance and x_{i1} and x_{i2} represent the attribute values of X_1 and X_2 at the i-th position, respectively.

The rules of the KNN graph algorithm are shown in eq 6

$$p(\overline{x},\ c_j) = \sum d_i \in \mathrm{KNN}(x)\mathrm{dist}(\overline{x},\ \overline{y_i})\delta(\overline{y_i},\ c_j) \tag{6}$$

https://doi.org/10.1021/acsomega.1c04393
ACS Omega 2021, 6, 31699−31715

where $\overline{x}$is the test sample, $\overline{y_i}$is the training sample, dist($\overline{x}$, $\overline{y_i}$) is the similarity between the two samples, and c_j is the set of neighborhood samples of $\overline{x}$, which belongs to category j. Generally, the attributes of samples are determined by eq 7

$$\delta(\overline{y_i}, c_j) = \begin{cases} 1 & \overline{y_i} \in c_i \\ 0 & \overline{y_i} \notin c_i \end{cases} \quad (7)$$

For a target point (center point) x_i, the nearest k points can be found by the KNN graph algorithm, and a local graph about the center point $x_i$can be established, as shown in Figure 7.

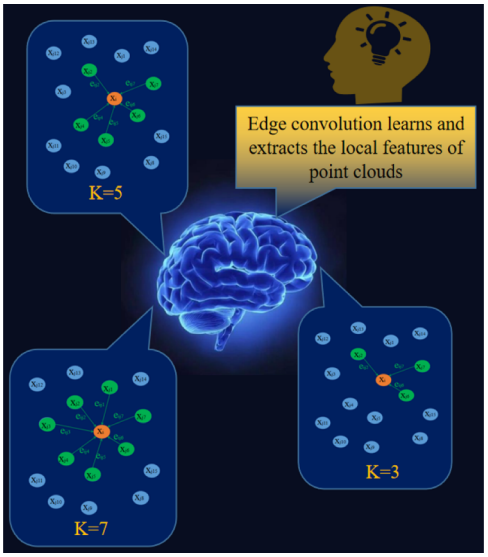

Figure 7. Different K values affect edge convolution to extract local features.

As shown in Figure 7, different K values directly affect the number of closest points and edge features of center point x_i in the current point cloud and then affect the feature aggregated by the center point. Therefore, in Section 3.4, we analyze the influence of different K values on the point cloud segmentation of the coal mine working face by DGCNNs.

2.4. Output Dimension of Edge Convolution. In DGCNNs, the input of the first edge convolution layer is a point cloud X composed of n points, which can be expressed by eq 8

$$X = (x_i \in R^F)_{i=1}^{n} \quad (8)$$

where X is the current point. F can include not only the 3D coordinates of each point but also the RGB information and normal information of each point. In this study, each point cloud only has 3D coordinate information, so F = 3. After edge convolution, the feature dimension of each point increases, as shown in Figure 8.

Figure 8 shows that after the edge convolution, the feature dimension information of the point cloud increases greatly so that the DGCNN model can learn the features of each point more abstractly. But very high feature dimension information will not necessarily have a good impact on the results.

According to the existing literature,[23,52] the higher the feature dimension of the point cloud is, the sparser the training data is and the lower the generalization ability of the model will be, and even cause an over fitting phenomenon, which will affect the performance of the network. The feature dimension

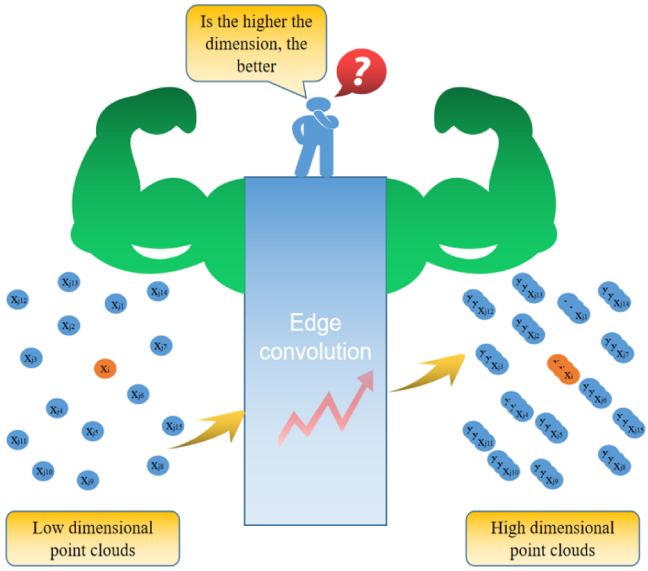

Figure 8. After edge convolution, the dimension of the point cloud increases.

of the point cloud cannot be too low because if the feature dimension of the point cloud is too low, the point cloud processed by the symmetric function will lose most of the information, thus affecting the effect of the network. It can be seen that it is very important to select the appropriate feature dimension of the point cloud. Therefore, this study analyzes the influence of the feature dimension of the point cloud output from edge convolution on the segmentation effect of DGCNNs in Section 3.5.

3. RESULTS AND DISCUSSION

3.1. Data Set Description. We make the data set according to the method described in Section 2.1 and take the point cloud of 0−300 m coal mine working face in the X direction as the training set and the point cloud of more than 300 m coal mine working face in the X direction as the test set. The number of point clouds of each category in the data set and the total number of point clouds of the coal mine working face are shown in Table 1.

Table 1. Number of Point Clouds in the Data Set

point cloud category	roof	coal wall	part of hydraulic support
number of point clouds	2,960,233	3,141,503	4,864,688
proportion (%)	26.993	28.647	44.360

The shearer in the coal mine working face mines along the X direction. Through Figure 4 of Section 2.1, we know that the range of the point cloud in the coal mine working face is large in the X direction and small in the Y and Z directions. In order to observe conveniently and intuitively the effect of point cloud segmentation by DGCNNs and other DNNs, we select a section of the point cloud test set of the coal mine working face for visualization (the range of the point cloud in the X direction is 320−330 m, the range in the Y direction is −3∼4 m, and the range in the Z direction is −0.5−1 m), as shown in Figure 9.

https://doi.org/10.1021/acsomega.1c04393
ACS Omega 2021, 6, 31699−31715

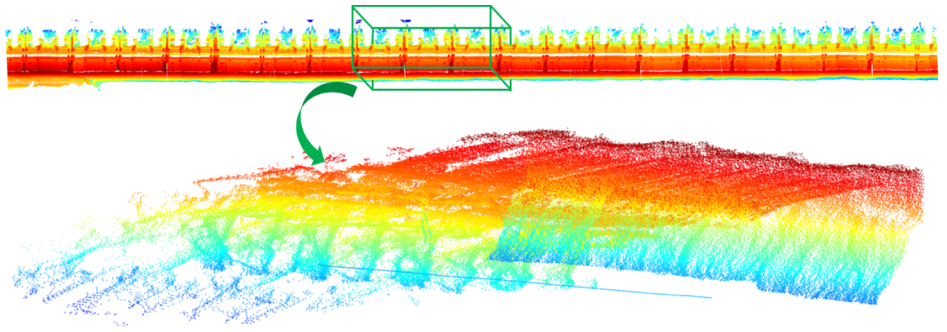

Figure 9. Visualization part of the test set of the point cloud in the coal mine working face.

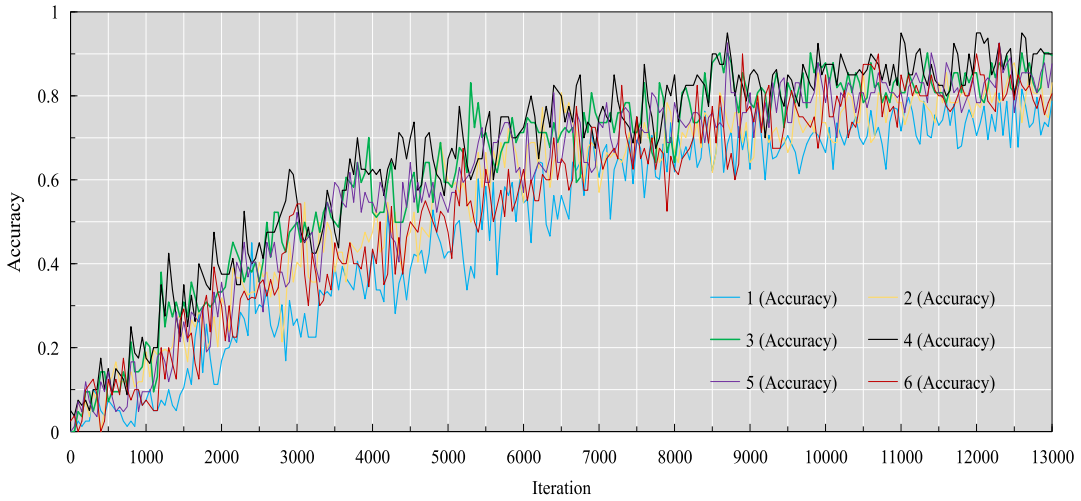

Figure 10. Accuracy of different numbers of edge convolution layers.

3.2. Experimental Details. The hardware configuration of our experimental workstation is as follows: CPU is Intel Core-I7 9700, GPU is NVIDIA GTX 2080 Super, and RAM is 16GB. Software configuration: TensorFlow 2.3.0 and Python 3.7.9.

We set the momentum to 0.9, batch size to 32, learning rate to 0.001, and dropout rate to 0.5. Rectified Linear Unit (ReLU) is selected as the activation function, and its expression is shown in eq 9.[53−55]

$$\mathrm{ReLU}(x) = \begin{cases} x & x \geq 0 \\ 0 & x < 0 \end{cases} \tag{9}$$

where x is the input of the upper network. The loss function is expressed as eq 10

$$L = -\sum_{i=1}^{N} y^{(i)} \log \hat{y}^{(i)} + (1 - \hat{y}^{(i)}) \log(1 - \hat{y}^{(i)}) \tag{10}$$

where N is the number of samples and y is the actual value of samples.

Compared with the object classification and recognition of the 3D point cloud, the segmentation of the 3D point cloud model needs to recognize the category of each point more precisely, which is a more challenging task. In order to obtain the intersection line of the coal wall and roof, we use different depth neural networks to segment the coal wall and the roof in the point cloud of the coal mine working face. Then, the point cloud coordinates on the intersection line of the coal wall and roof are obtained by fitting the point cloud. We use accuracy to evaluate the segmentation effect of the DNN and analyze the ability of different depth neural network models to deal with 3D point cloud fine-grained tasks. The expression of accuracy is as eq 11

$$\text{accuracy} = \frac{\mathrm{TP} + \mathrm{TN}}{\mathrm{TP} + \mathrm{FP} + \mathrm{TN} + \mathrm{FN}} \tag{11}$$

where TP is the number of correctly divided positive cases, FP is the number of wrongly divided positive cases, FN is the number of wrongly divided negative cases, and TN is the number of correctly divided negative cases.

The point cloud coordinates on the actual intersection line of the coal wall and the roof have been manually obtained and marked with the assistance of Matlab R2019a software. We use the average error to evaluate the intersection line results obtained by segmenting the point cloud with different depth neural networks. The calculation equation for the average error of the corresponding point cloud on the intersection line is eq 12

$$\text{error} = \frac{\sum_{i=1}^{n} \sqrt{(x_{mi} - x_{ri})^2 + (y_{mi} - y_{ri})^2 + (z_{mi} - z_{ri})^2}}{n} \tag{12}$$

where n is the number of point clouds on the current intersection line, x_m, y_m, and z_m correspond to the 3D coordinates of the point clouds on the intersection line found by the depth neural network, respectively, and x_r, y_r, and z_r correspond to the actual 3D coordinates of the point clouds on the intersection line, respectively.

https://doi.org/10.1021/acsomega.1c04393
ACS Omega 2021, 6, 31699−31715

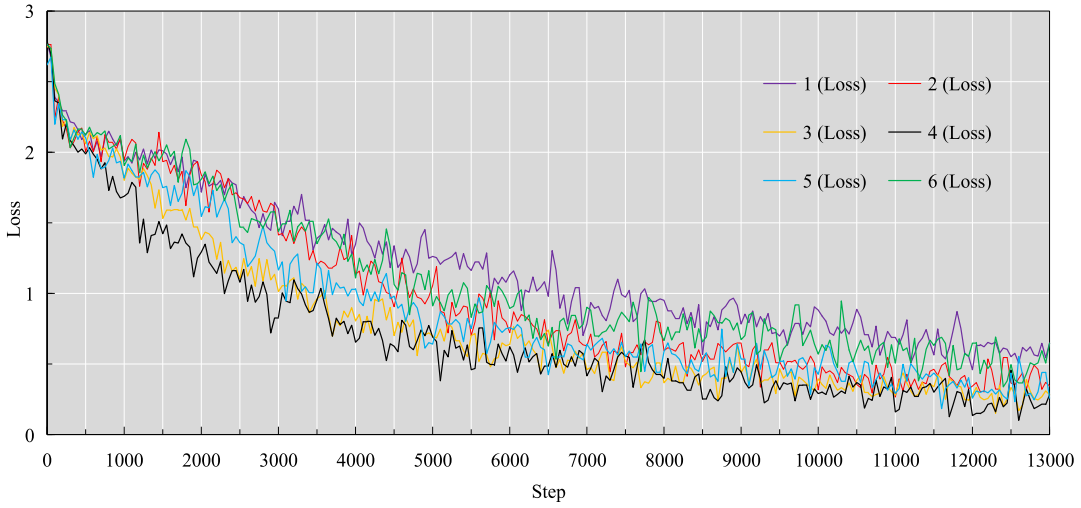

Figure 11. Loss of different numbers of edge convolution layers.

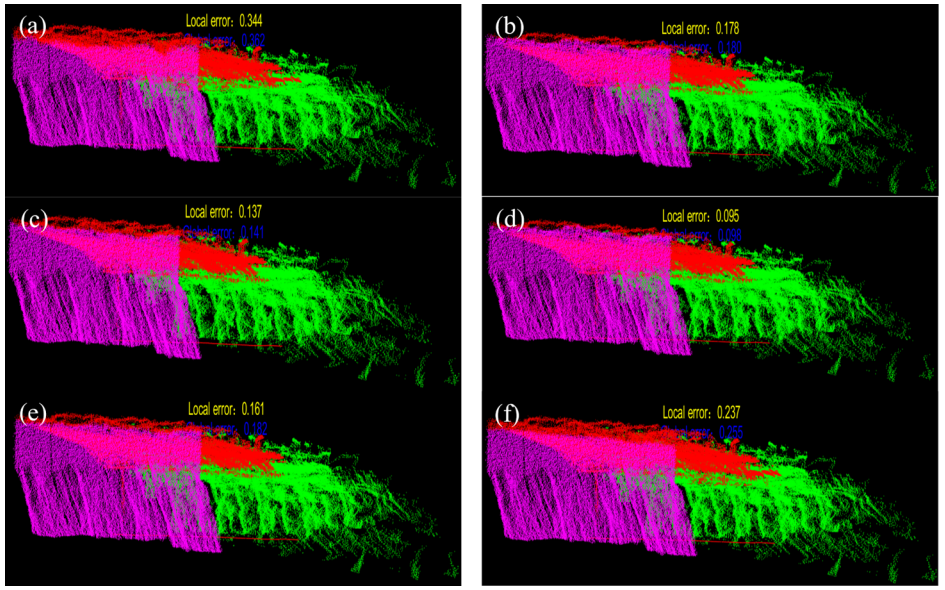

Figure 12. Segmentation effect and intersection line error of the point cloud in the coal mine working face. (a) Number of edge convolution layers is one, (b) number of edge convolution layers is two, (c) number of edge convolution layers is three, (d) number of edge convolution layers is four, (e) number of edge convolution layers is five, and (f) number of edge convolution layers is six.

3.3. Results of Different Number of Edge Convolution Layers. The different structures of the neural network will affect the segmentation effect of the point cloud in the coal mine working face, which directly affects the error between the intersection line obtained by the neural network and the real intersection line. We have obtained the accuracy and loss of the point cloud of the coal mine working face segmented by DGCNNs under different numbers of edge convolution layers, as shown in Figures 10 and 11.

As shown in Figures 10 and 11, when the number of edge convolution layers is four, the accuracy of DGCNNs is the largest and the loss is the smallest. With the increase of the number of edge convolution layers, the accuracy first increases and then decreases, and the loss first decreases and then increases. The reason for the abovementioned phenomenon is that the edge convolution in DGCNNs can make the center point continuously aggregate the neighbor information nearby, which makes DGCNNs better complete the fine-grained task of the point cloud. However, when the number of edge convolution layers increases to a certain number, the aggregated information of each point cloud will be too smooth, which will affect the segmentation effect of DGCNNs. Even if there is no limit on the number of edge convolution layers, each point will aggregate the global information, and the representation of all points will converge to a fixed point.

Under the DGCNN model of different numbers of edge convolution layers, we visualize the segmentation effect of the coal wall and the roof in the point cloud of the coal mine working face and obtain the change of the intersection line error, as shown in Figure 12. Among them, the point cloud of the coal wall is magenta, the point cloud of the roof is red, and the point cloud of part of hydraulic support is green. The yellow number at the top of the figure is the average error of the intersection line within the selected range, and the blue number is the average error of the intersection line of the coal mine working face corresponding to the whole test set.

From Figure 12, we can see that when the number of edge convolution layers is four, the local error and global error are

https://doi.org/10.1021/acsomega.1c04393
ACS Omega 2021, 6, 31699−31715

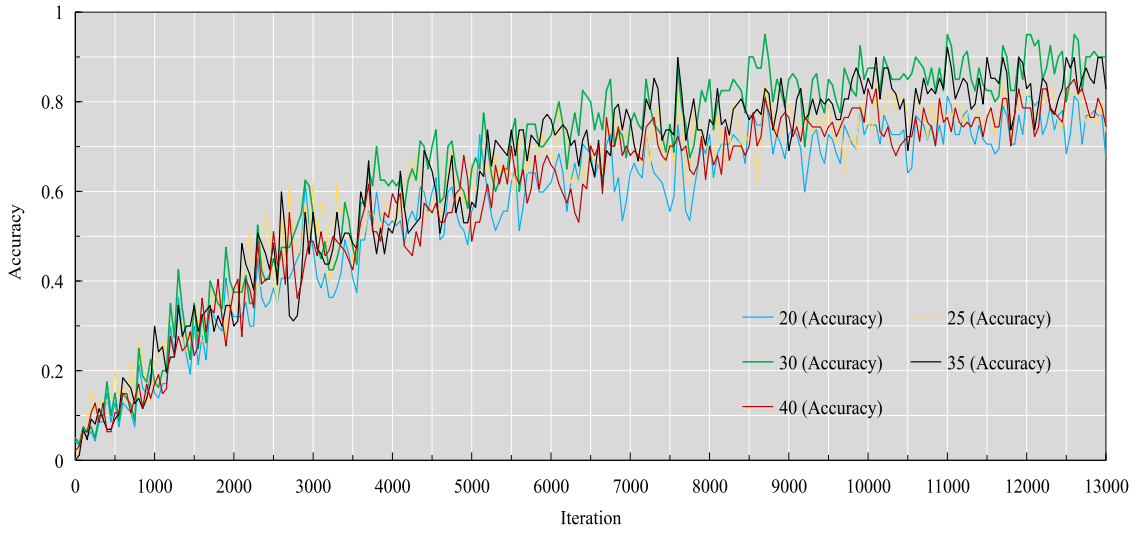

Figure 13. Accuracy with different *K* values.

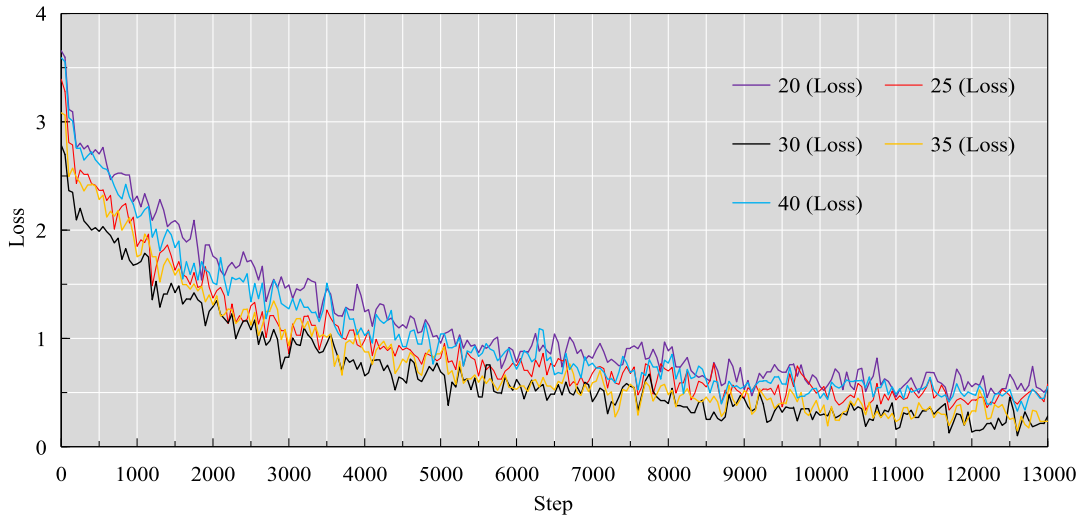

Figure 14. Loss of different *K* values.

the smallest. It shows the correctness of the number of edge convolution layers we selected in the point cloud segmentation of the coal mine working face. The less the number of edge convolution layers, the better. Regarding accuracy and loss, with the increase of the number of edge convolution layers, accuracy first increases and then decreases, loss first decreases and then increases, and the segmentation result changes from bad to good and then to bad. With the increase of the number of edge convolution layers, the local error and global error of the intersection line under different numbers of edge convolution layers first decrease and then increase, and the result also changes from bad to good and then to bad. After stacking a large number of network layers, the general deep learning model will achieve better results because of its strong representation ability. While, in the DGCNN, after stacking a small number of edge convolution layers, the network achieves the best effect. If the DGCNN continues to increase the number of edge convolution layers, the result will become worse because edge convolution contains the operation of aggregating the features of neighbor points. By increasing the number of edge convolution layers, the center point can potentially represent the information features of points far from the center point and then fully and effectively describe the local features. When the number of edge convolution layers increases to a certain number, the aggregated information of each point will be too smooth, that is, there is no obvious discrimination of each point, which will affect the segmentation effect of the DGCNN and then affect the local error and global error of the intersection line.

According to the abovementioned research, the number of edge convolution layers in the DGCNN cannot be too much or too little. Because the intersection line of the coal wall and roof can reflect the direction information of the scraper conveyor, we hope that the smaller the error of the intersection line, the better so as to provide a more accurate data basis for the straightening of the scraper conveyor. Therefore, in addition to improving the number of edge convolution layers, how to further reduce the error is one of the main research directions in our future work.

3.4. Comparison of Different *K* Values. After elucidating the influence of the layer number of edge convolution layers on the point cloud of the coal mine working face segmented by DGCNNs, we analyze the accuracy and loss of DGCNNs with

https://doi.org/10.1021/acsomega.1c04393
ACS Omega 2021, 6, 31699−31715

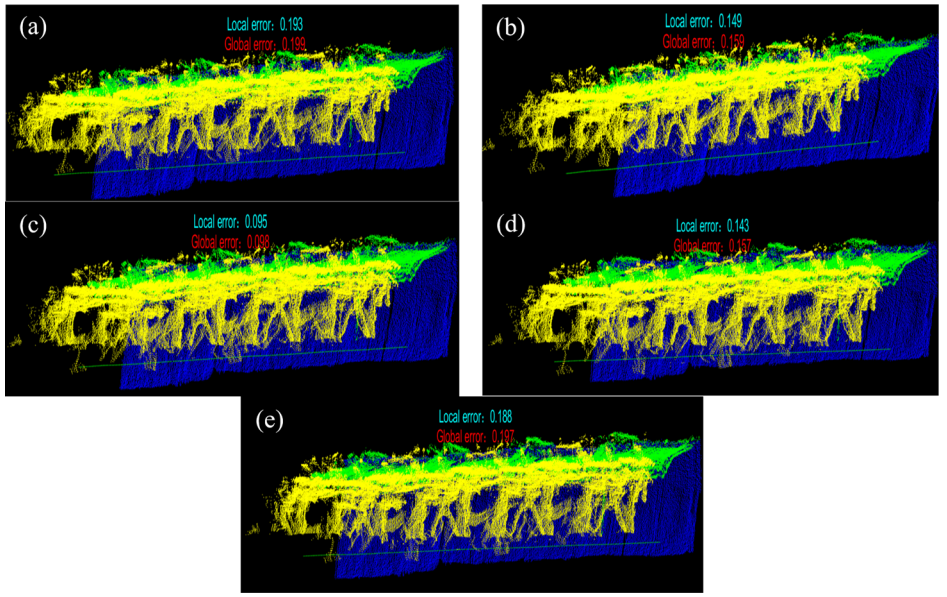

Figure 15. Point cloud segmentation effect and intersection line error in the coal mine working face under different K values. (a) K value is 20, (b) K value is 25, (c) K value is 30, (d) K value is 35, and (e) K value is 40.

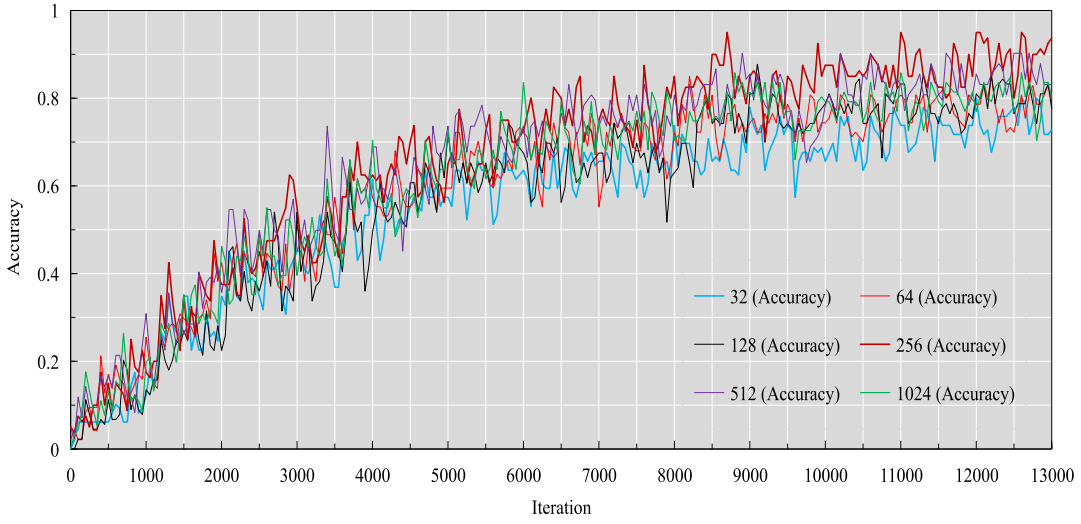

Figure 16. Accuracy of different feature dimensions.

different K values of the KNN graph algorithm in edge convolution, as shown in Figures 13 and 14.

As shown in Figures 13 and 14, when the K value is 30, the maximum accuracy and the minimum loss are obtained, and the segmentation performance of the DGCNN is the best. With the increase of the K value, the accuracy first increases and then decreases, and the loss first decreases and then increases. The reason for this phenomenon is that when the K value is too small, the receptive field of edge convolution is too small, and the DGCNN cannot effectively describe the local fine-grained feature; therefore, it cannot fully learn the local feature of the point cloud in the coal mine working face. When the K value is too large, the DGCNN ignores the global information and falls into the learning of local details of the point cloud in the coal mine working face.

Under different K values, the visualization of the DGCNN segmentation point cloud of the coal mine working face and the local error and global error of the intersection line are shown in Figure 15.

As shown in Figure 15, the point cloud of the coal wall is blue, the point cloud of the roof is green, and the point cloud of part of hydraulic support is yellow. The cyan number at the top of the figure is the average error of the intersection line within the selected range of visualization, and the red number is the average error of the intersection line of the coal mine working face corresponding to the whole test set. We find that when the K value is 30, the accuracy of the DGCNN is the largest and the loss of the DGCNN is the smallest, and we get the best segmentation effect. When K is 30, the local error and global error of the intersection line are the smallest whether in the coal mine working face point cloud of the visual local section or in the coal mine working face point cloud of the whole test set. When K is greater than 30 or K is less than 30, the accuracy decreases and the loss, local error, and global error increase. The abovementioned results show the correctness of selecting a K value of 30 when segmenting the coal mine working face point cloud. From this phenomenon, we also find that the K value affects the range of the receptive field

https://doi.org/10.1021/acsomega.1c04393
ACS Omega 2021, 6, 31699−31715

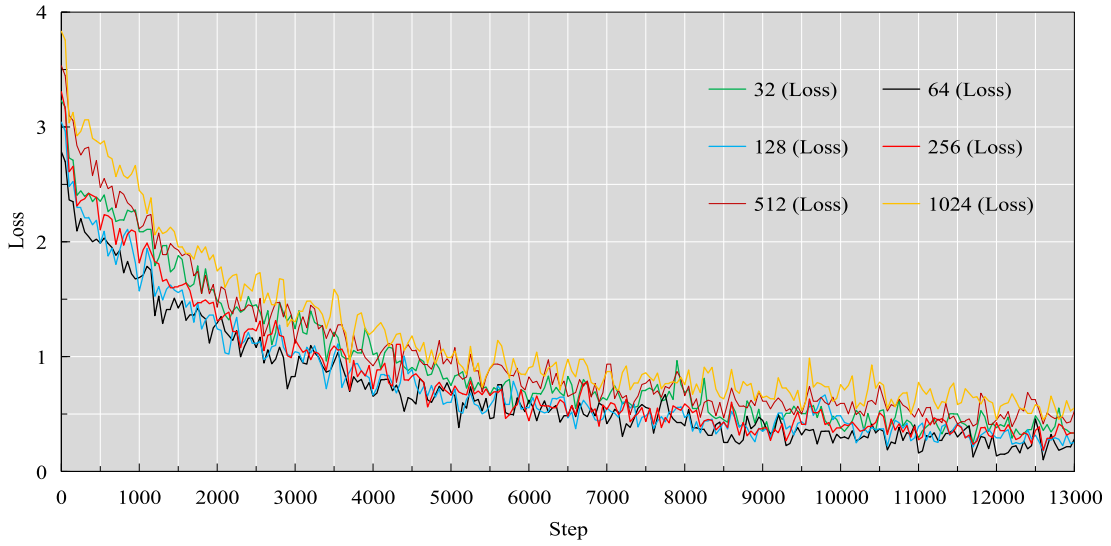

Figure 17. Loss of different feature dimensions.

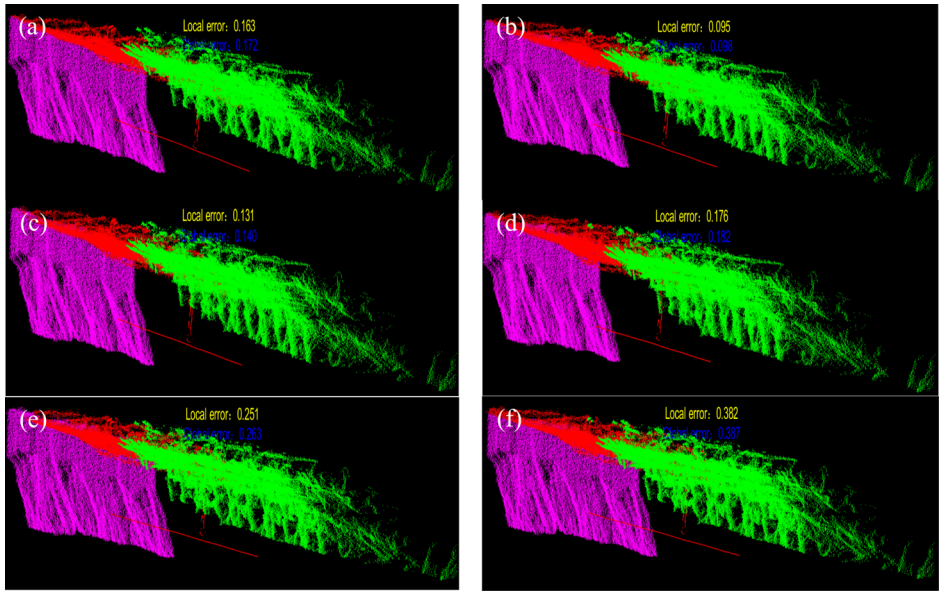

Figure 18. Segmentation effect and the intersection line error of the coal mine working face under different dimensions. (a) Dimension is 32, (b) dimension is 64, (c) dimension is 128, (d) dimension is 256, (e) dimension is 512, and (f) dimension is 1024.

of edge convolution in the DGCNN. By increasing the *K* value, the center point can aggregate more information of neighbor points. The DGCNN can more fully learn the local features of the point cloud in the coal mine working face and then improve the segmentation effect of the point cloud in the coal mine working face. However, when the *K* value is too large, the central point looks for too many neighbor points to build the local graph of the central point, which leads to the decline of the segmentation effect of the point cloud in the coal mine working face. The DGCNN learns the features of the coal mine working face point cloud in a large neighborhood, which makes the overall model simple, falls into the learning of local details of the point cloud, and finally affects the performance of the DGCNN.

3.5. Comparison of Different Dimensions. We analyze the influence of different feature dimensions on the accuracy and loss of the DGCNN, as shown in Figures 16 and 17.

Figures 16 and 17 show that under the current point cloud data of the coal mine working face, when the output dimension of edge convolution is 64, the DGCNN has the maximum accuracy and the minimum loss. When the output dimension of edge convolution is 32, the DGCNN has the minimum accuracy and the maximum loss. When the dimension is 64, not only the parameters of the DGCNN model are low but also the network performance is maintained. In addition, we can see that with the increase of the dimension, accuracy first increases and then decreases and loss first decreases and then increases. The reason for the abovementioned phenomenon is that in this study, the data structure of the point cloud is a set of coordinates of points in 3D space, and the amount of information that the point cloud can provide is relatively limited. Through the dimension elevation of the point cloud, the information loss of the point cloud processed by the symmetric function can be avoided, and the DNN can learn the features of the point cloud more deeply. However, in a

https://doi.org/10.1021/acsomega.1c04393
ACS Omega 2021, 6, 31699−31715

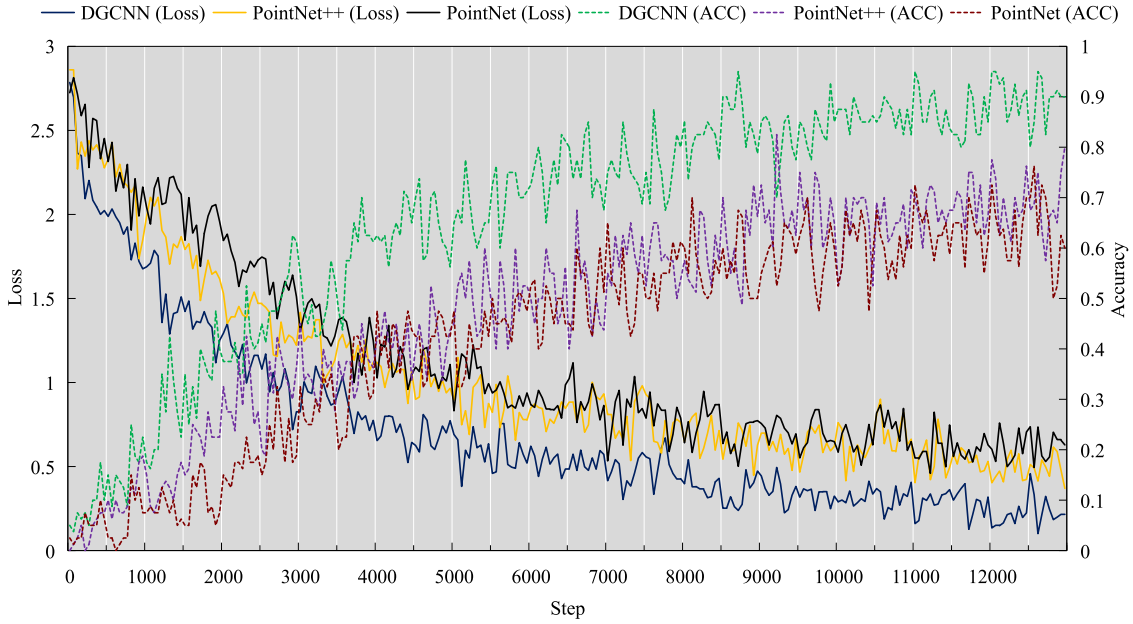

Figure 19. Accuracy and loss of different networks.

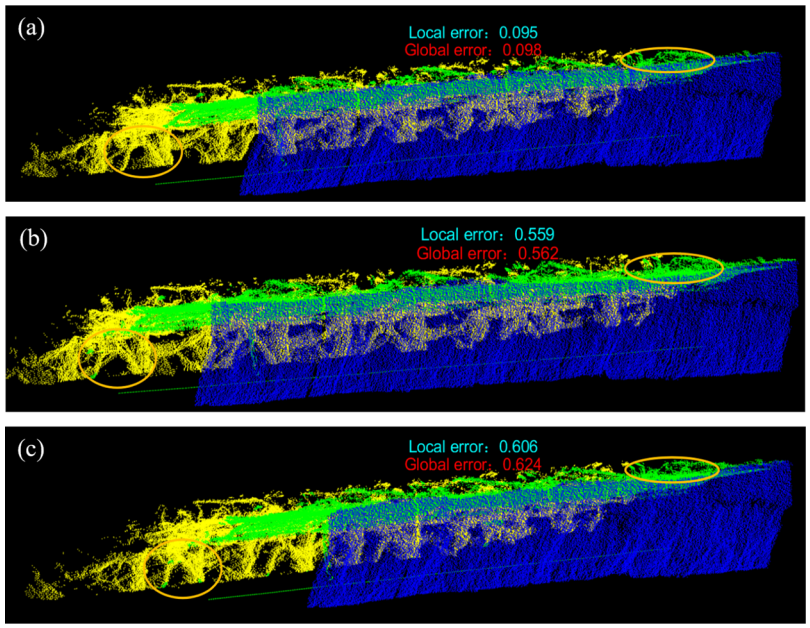

Figure 20. Results of different depth neural network models. (a) Ours, (b) PointNet++, and (c) PointNet.

certain data set, too much feature dimension of the point cloud is not beneficial to the expression and learning of the point cloud model, which not only increases the complexity of the network but also leads to smaller and smaller sample density and reduces the generalization ability of the model, and even causes the over fitting phenomenon, which affects the performance of the network.

Under the different feature dimensions of the output of the edge convolution, we visualize the segmentation effect of the point cloud of the coal mine working face by the DGCNN and show the intersection line error, as shown in Figure 18.

As shown in Figure 18, the point cloud of the coal wall is magenta, the point cloud of the roof is red, and the point cloud of part of hydraulic support is green. The yellow number at the top of the figure is the average error of the intersection line within the selected range, and the blue number is the average error of the intersection line of the coal mine working face corresponding to the whole test set. We find that when the dimension is 64, not only the accuracy of the DGCNN is the largest and the loss of the DGCNN is the smallest but also the local error and global error of the intersection line are the smallest. After edge convolution, we increase the dimension of the point cloud with only 3D coordinate information to 64, so that the DGCNN model can learn the features of each point more abstractly, and obtain the best segmentation effect and the most accurate intersection line. In addition, with the increase of the dimension of the point cloud, the accuracy first increases and then decreases, the loss first decreases and then increases, and the local error and global error first increase and then decrease. Very high feature dimension information may

https://doi.org/10.1021/acsomega.1c04393
ACS Omega 2021, 6, 31699−31715

not have a good impact on the results. This is because under the current coal mine working face point cloud data set, the more the feature dimensions of the point cloud, the more sparse the training data. On the one hand, it will make the network appear bloated, on the other hand, it will reduce the generalization ability of the model, which will affect the performance of the network. However, the DGCNN needs to use the symmetry function to ensure the disorder of the point cloud. When the feature dimension of the point cloud does not rise to a certain extent, the feature dimension of the point cloud is relatively low. The point cloud processed by the symmetric function will lose most of the information, which will also affect the segmentation effect of the DGCNN and the accurate acquisition of the intersection line.

3.6. Comparison of Different Networks. At present, no researchers have used DNNs to segment the point cloud of the coal mine working face, and no researchers have obtained the intersection line of the coal wall and roof point cloud. The research in these two aspects is blank. Therefore, we specially built PointNet and PointNet++ models and then compared them with DGCNNs, which determines the number of layers, K values, and output feature dimensions of edge convolution. The accuracy, loss, local error, and global error of the intersection line are analyzed, and the experimental results are deeply studied. The accuracy and loss of DGCNNs, PointNet, and PointNet++ in segmenting the same coal mine working face point cloud are shown in Figure 19.

Figure 19 shows that the accuracy of the DGCNN is greater than the corresponding results of PointNet and PointNet++, and the loss of the DGCNN is less than the corresponding results of PointNet and PointNet++. The DGCNN shows the best performance. The reason for the abovementioned results is that PointNet extracts the features of each point independently, without considering the information of local neighbor points, resulting in the lack of learning local features of the point cloud and the loss of local features of the point cloud. Although PointNet++ samples point clouds on the basis of PointNet, PointNet++ uses PointNet as a regional feature extractor to extract and integrate local features of point clouds into global features layer by layer, which means that in the process of point cloud segmentation, PointNet is still used in PointNet++. The features of the point cloud are extracted separately, and the learning of local features is still insufficient.

We visualize the results of point cloud segmentation of the coal mine working face with different depth neural network models and display the local error and global error of the intersection line at the same time, as shown in Figure 20.

As shown in Figure 20, the point cloud of the coal wall is blue, the point cloud of the roof is green, and the point cloud of part of hydraulic support is yellow. The cyan number at the top of the figure is the average error of the intersection line within the selected range of visualization, and the red number is the average error of the intersection line of the coal mine working face corresponding to the whole test set. It can be seen that the local error and global error obtained by the DGCNN are far lower than the corresponding results of PointNet and PointNet++, showing the best performance. PointNet constructs a DNN structure that can directly input the 3D disordered point cloud and output the classification results of the whole point cloud or the segmentation label of each point. Although PointNet has pioneering achievements in directly extracting point cloud features, PointNet learns the corresponding spatial code for each point in the input point cloud and then directly and violently pools all points into a global feature, which does not consider the local feature information of point cloud data. PointNet++ is an improved version of PointNet. PointNet++ uses PointNet to extract the features of local areas of the point cloud iteratively so that it can learn the features with larger and larger local scale, which makes up for the lack of local feature extraction by PointNet and the low accuracy of PointNet in processing uneven point cloud scenes. However, PointNet is still used in PointNet++, which means that the features of the point cloud are extracted separately in the sampling area, and the learning of local features is still insufficient. Therefore, PointNet and PointNet++ misjudge the point cloud of the coal wall, roof, and part of hydraulic support in many places; we have highlighted the more obvious places with orange ellipses.

DGCNNs can effectively overcome the abovementioned shortcomings. On the one hand, the DGCNN selects K neighbor points in the feature space, and the calculated features of each layer are different, that is, the connection relationship of the graph is learned by the network itself, which is equivalent to that the graph of each layer has different vertices, and the maximum receptive field of edge convolution can reach the diameter of the whole point cloud. On the other hand, edge convolution is mainly used to extract the local features of the point cloud, which makes up for the lack of local information of the point cloud in the process of direct extraction of point cloud features by the DNN. In the DGCNN, each point in the point cloud is independent of each other in the process of calculating features, which is the extraction of global features. In addition, for each point in the point cloud data, the DGCNN considers not only the features of the current point but also the features of the K points closest to the central point in the current feature space, which shows that the local features of the point cloud can be extracted from the local graph composed of K points. In the point cloud of the coal mine working face, it is difficult to distinguish these three kinds of point clouds by simply extracting the features of the point cloud of the coal wall, roof, and hydraulic support. However, the extension of the coal wall, roof, and hydraulic support in their respective directions is quite different. Therefore, the DGCNN can better distinguish these three kinds of point clouds in combination with its contextual point cloud information.

In addition, edge convolution in the DGCNN does not directly aggregate the feature information of local neighbor points but uses the connecting edge between two interconnection points to represent the feature information synthesis of two interconnection points. Edge convolution constructs a local edge relation feature graph based on the center point and learns the edge elements of each neighbor point. The DGCNN takes into account the neighborhood information of the point cloud; therefore, the DGCNN studied in this paper performs better than PointNet and PointNet++ in segmenting the point cloud of the coal mine working face. The abovementioned results show that it is feasible and correct for us to use DGCNNs to further study the point cloud of the coal mine working face and provide an important premise and reference for DGCNNs to achieve good application results in the field of energy and geology.

4. CONCLUSIONS

Coal is an important raw material for the chemical industry and metallurgy. The intelligent coal mine working face is

https://doi.org/10.1021/acsomega.1c04393
ACS Omega 2021, 6, 31699−31715

imperative. Segmenting the point cloud of the coal mine working face and then obtaining the intersection line of the point cloud of the coal wall and the roof can provide a direct basis for the intelligent straightening and inclination adjustment of the scraper conveyor. However, the direct and indirect point cloud segmentation methods based on deep learning have their own shortcomings. We propose using DGCNNs to segment the point cloud of the coal mine working face and analyze the influence of edge convolution (the greatest innovation of DGCNNs) on the network results in many aspects. First of all, we make and batch label the point cloud of the coal mine working face, which fills the blank of the data set in this aspect. Also, we randomly select a certain range of the point cloud within the range of 0−300 m in the X direction, so we need not divide the point cloud into multiple training data, which effectively and easily realizes the DNN model to learn the feature of the point cloud of the coal mine working face. Second, edge convolution can make DGCNNs better complete the fine-grained task of the point cloud, but when the number of edge convolution layers increases to a certain number, the aggregated information of each point cloud will be too smooth, which will affect the effect of point cloud segmentation by DGCNNs. Therefore, we analyze the optimal number of edge convolution layers for the DGCNN to segment the point cloud of the coal mine working face, and we know that when the edge convolution layer is four, the DGCNN obtained the minimum loss, the minimum intersection line error, and the maximum accuracy. At the same time, the K value inside the edge convolution and the feature dimension of the point cloud output from the edge convolution are studied. We find that in the point cloud of the coal mine working face segmented by the DGCNN, the larger K value and the feature dimension are not necessarily the better. Finally, we compare the improved DGCNN with PointNet and PointNet++. The results show that the DGCNN shows the best performance in both the whole test set and the local section of the point cloud in the coal mine working face. It shows the feasibility and correctness of using DGCNNs to segment the point cloud of the coal mine working face. The results provide a direct basis for the straightening and inclining adjustment of the scraper conveyor and provide a key premise for the intelligent height adjustment of the shearer. It is of great significance for the realization of an intelligent coal mine working face. In addition, the research results are of great help to promote the safe and efficient mining of coal and to reduce the accident rate caused by harmful gases such as CO produced by spontaneous combustion of coal and other factors.

Last but not least, the research team of the author has installed an expensive underground inspection robot to collect the point cloud of the coal mine working face. According to the previous research results, the markers in the point cloud of the coal mine working face can be found through DGCNNs. This study has conducted further in-depth exploration and has learned that DGCNNs can accurately segment the point cloud of the coal mine working face and obtain the intersection line of the coal wall and roof. The research results provide a premise for DGCNNs to achieve a good application effect in the field of energy. In the future work, we will further study the structure of DGCNNs so that it can maintain excellent performance in dealing with more and different tasks and make our contribution to the application of DGCNNs.

AUTHOR INFORMATION

Corresponding Author

Shuanfeng Zhao − *College of Mechanical Engineering, Xi'an University of Science and Technology, Xi'an 710054, China;* orcid.org/0000-0002-3027-223X; Email: zsf@xust.edu.cn

Authors

Zhizhong Xing − *College of Mechanical Engineering, Xi'an University of Science and Technology, Xi'an 710054, China;* orcid.org/0000-0002-8674-7433

Wei Guo − *College of Mechanical Engineering, Xi'an University of Science and Technology, Xi'an 710054, China*

Xiaojun Guo − *School of Mechanical & Automotive Engineering, South China University of Technology, Guangzhou 510641, China*

Shenquan Wang − *College of Mechanical Engineering, Xi'an University of Science and Technology, Xi'an 710054, China*

Junjie Ma − *College of Mechanical Engineering, Xi'an University of Science and Technology, Xi'an 710054, China*

Haitao He − *College of Mechanical Engineering, Xi'an University of Science and Technology, Xi'an 710054, China; Shendong Coal Group Co., Ltd. of National Energy Group, Yulin 719315, China*

Complete contact information is available at: https://pubs.acs.org/10.1021/acsomega.1c04393

Notes

The authors declare no competing financial interest.

ACKNOWLEDGMENTS

This study was supported by the National Key R&D Program of China (grant no. 2017YFC0804310) and the Key R&D Projects of Shaanxi Province (Grant Nos. 2019ZDLGY03-09-02, 2020ZDLGY04-05, and 2020ZDLGY04-06). The authors thank the reviewers and editors for their constructive comments and suggestions on improving this manuscript. The authors thank Ying Yang of Xi'an International Studies University for polishing the wording of the manuscript.

REFERENCES

(1) Oberschelp, C.; Pfister, S.; Raptis, C. E.; Hellweg, S. Global Emission Hotspots of Coal Power Generation. *Nat. Sustain* **2019**, *2*, 113−121.

(2) Zhao, H.; Tian, X.; Ma, J.; Chen, X.; Su, M.; Zheng, C.; Wang, Y. Chemical Looping Combustion of Coal in China: Comprehensive Progress, Remaining Challenges, and Potential Opportunities. *Energy Fuels* **2020**, *34*, 6696−6734.

(3) Ding, J.; Zhou, G.; Liu, D.; Jiang, W.; Wei, Z.; Dong, X. Synthesis and Performance of a Novel High-Efficiency Coal Dust Suppressant Based on Self-Healing Gel. *Environ. Sci. Technol.* **2020**, *54*, 7992−8000.

(4) Han, W.; Zhou, G.; Zhang, Q.; Pan, H.; Liu, D. Experimental study on modification of physicochemical characteristics of acidified coal by surfactants and ionic liquids. *Fuel* **2020**, *266*, 116966.

(5) Tutak, M.; Brodny, J. Forecasting Methane Emissions from Hard Coal Mines Including the Methane Drainage Process. *Energies* **2019**, *12*, 3840.

(6) Zhu, T.; Bian, W.; Zhang, S.; Di, P.; Nie, B. An Improved Approach to Estimate Methane Emissions from Coal Mining in China. *Environ. Sci. Technol.* **2017**, *51*, 12072−12080.

(7) Yang, Q.; Li, X.; Yang, Q.; Huang, W.; Yu, P.; Zhang, D. Opportunities for CO2 Utilization in Coal to Green Fuel Process:

Optimal Design and Performance Evaluation. *ACS Sustainable Chem. Eng.* **2020**, *8*, 1329−1342.
(8) Einicke, G. A.; Ralston, J. C.; Hargrave, C.; Reid, D. C.; Hainsworth, D. Longwall mining automation an application of minimum-variance smoothing. *IEEE Control Syst.* **2020**, *28*, 28−37.
(9) Yang, H.; Li, W.; Luo, T.; Liang, H.; Zhang, H.; Gu, Y.; Luo, C. Research on the Strategy of Motion Constraint-Aided ZUPT for the SINS Positioning System of a Shearer. *Micromachines* **2017**, *8*, 340.
(10) Fan, Q.; Li, W.; Hui, J.; Wu, L.; Yu, Z.; Yan, W.; Zhou, L. Integrated positioning for coal mining machinery in enclosed underground mine based on SINS/WSN. *Sci. World J.* **2014**, *2014*, 1−12.
(11) Bai, X.; Wen, W.; Hsu, L.-T. Robust Visual-Inertial Integrated Navigation System Aided by Online Sensor Model Adaption for Autonomous Ground Vehicles in Urban Areas. *Remote Sens.* **2020**, *12*, 1686.
(12) Chung, H.; Miller, O. D. Tunable Metasurface Inverse Design for 80% Switching Efficiencies and 144° Angular Deflection. *ACS Photonics* **2020**, *7*, 2236−2243.
(13) Scheuer, J. Optical Metasurfaces Are Coming of Age: Short- and Long-Term Opportunities for Commercial Applications. *ACS Photonics* **2020**, *7*, 1323−1354.
(14) Tyner, D. R.; Johnson, M. R. Where the Methane Is—Insights from Novel Airborne LiDAR Measurements Combined with Ground Survey Data. *Environ. Sci. Technol.* **2021**, *55*, 9773−9783.
(15) Schnell, M.; Goikoetxea, M.; Amenabar, I.; Carney, P. S.; Hillenbrand, R. Rapid Infrared Spectroscopic Nanoimaging with nano-FTIR Holography. *ACS Photonics* **2020**, *7*, 2878−2885.
(16) Van Oosterom, P.; Dimopoulou, E. Introduction to the Special Issue: "Research and Development Progress in 3D Cadastral Systems". *ISPRS Int. J. Geo-Inf.* **2018**, *7*, 59.
(17) Ayanu, Y. Z.; Conrad, C.; Nauss, T.; Wegmann, M.; Koellner, T. Quantifying and Mapping Ecosystem Services Supplies and Demands: A Review of Remote Sensing Applications. *Environ. Sci. Technol.* **2012**, *46*, 8529−8541.
(18) Liu, Y.; Sarnat, J. A.; Kilaru, V.; Jacob, D. J.; Koutrakis, P. Estimating Ground-Level PM2.5 in the Eastern United States Using Satellite Remote Sensing. *Environ. Sci. Technol.* **2005**, *39*, 3269−3278.
(19) Woo, H.; Kang, E.; Wang, S.; Lee, K. H. A New Segmentation Method for Point Cloud Data. *Int. J. Mach. Tool Manufact.* **2002**, *42*, 167−178.
(20) Limberger, F. A.; Oliveira, M. M. Real-time detection of planar regions in unorganized point clouds. *Pattern Recogn.* **2015**, *48*, 2043−2053.
(21) Sampath, A.; Jie Shan, J. Segmentation and reconstruction of polyhedral building roofs from aerial lidar point clouds. *IEEE Trans. Geosci. Electron.* **2010**, *48*, 1554−1567.
(22) Yang, H.; Wang, Z.; Lin, L.; Liang, H.; Huang, W.; Xu, F. Two-Layer-Graph Clustering for Real-Time 3D LiDAR Point Cloud Segmentation. *Appl. Sci.* **2020**, *10*, 8534.
(23) Blanc, T.; El Beheiry, M.; Caporal, C.; Masson, J.-B.; Hajj, B. Genuage: Visualize and Analyze Multidimensional Single-molecule Point Cloud Data in Virtual Reality. *Nat. Methods* **2020**, *17*, 1100−1102.
(24) Tachella, J.; Altmann, Y.; Mellado, N.; McCarthy, A.; Tobin, R.; Buller, G.; Tourneret, J.; McLaughlin, S. Real-time 3D Reconstruction From Single-photon Lidar Data Using Plug-and-play Point Cloud Denoisers. *Nat. Commun.* **2019**, *10*, 4984.
(25) Shi, L.; Li, B.; Kim, C.; Kellnhofer, P.; Matusik, W. Towards Real-time Photorealistic 3D Holography with Deep Neural Networks. *Nature* **2021**, *591*, 234−239.
(26) Chizhik, A. M.; Ruhlandt, D.; Pfaff, J.; Karedla, N.; Chizhik, A. I.; Gregor, I.; Kehlenbach, R. H.; Enderlein, J. Three-Dimensional Reconstruction of Nuclear Envelope Architecture Using Dual-Color Metal-Induced Energy Transfer Imaging. *ACS Nano* **2017**, *11*, 11839−11846.
(27) Zhu, L.; Kukko, A.; Virtanen, J.-P.; Hyyppä, J.; Kaartinen, H.; Hyyppä, H.; Turppa, T. Multisource Point Clouds, Point Simplification and Surface Reconstruction. *Remote Sens.* **2019**, *11*, 2659.
(28) Kim, Y.; Yang, C.; Kim, Y.; Gu, G. X.; Ryu, S. Designing an Adhesive Pillar Shape with Deep Learning-Based Optimization. *ACS Appl. Mater. Interfaces* **2020**, *12*, 24458−24465.
(29) Hu, J.; Liu, T.; Choo, P.; Wang, S.; Reese, T.; Sample, A. D.; Odom, T. W. Single-Nanoparticle Orientation Sensing by Deep Learning. *ACS Cent. Sci.* **2020**, *6*, 2339−2346.
(30) Liu, T.; de Haan, K.; Bai, B.; Rivenson, Y.; Luo, Y.; Wang, H.; Karalli, D.; Fu, H.; Zhang, Y.; FitzGerald, J.; Ozcan, A. Deep Learning-Based Holographic Polarization Microscopy. *ACS Photonics* **2020**, *7*, 3023−3034.
(31) Shin, H.; Oh, S.; Hong, S.; Kang, M.; Kang, D.; Ji, Y.-g.; Choi, B. H.; Kang, K.-W.; Jeong, H.; Park, Y.; Hong, S.; Kim, H. K.; Choi, Y. Early-Stage Lung Cancer Diagnosis by Deep Learning-Based Spectroscopic Analysis of Circulating Exosomes. *ACS Nano* **2020**, *14*, 5435−5444.
(32) Grambow, C. A.; Pattanaik, L.; Green, W. H. Deep Learning of Activation Energies. *J. Phys. Chem. Lett.* **2020**, *11*, 2992−2997.
(33) Sung, M.; Kim, J.; Cho, H.; Lee, M.; Yu, S.-C. Underwater-Sonar-Image-Based 3D Point Cloud Reconstruction for High Data Utilization and Object Classification Using a Neural Network. *Electronics* **2020**, *9*, 1763.
(34) Castaño, F.; Beruvides, G.; Villalonga, A.; Haber, R. Self-Tuning Method for Increased Obstacle Detection Reliability Based on Internet of Things LiDAR Sensor Models. *Sensors* **2018**, *18*, 1508.
(35) Kainz, W.; Tang, X.; Xue, Y. The Austrian node of the natural resources satellite remote sensing cloud service platform: examples of Sino-Austrian cooperation. *Geo Spat Inf Sci* . **2021**, *24*, 145−151.
(36) Lawin, F. J.; Danelljan, M.; Tosteberg, P.; Bhat, G.; Khan, F. S.; Felsberg, M. Deep projective 3D semantic segmentation. *International Conference on Computer Analysis of Images and Patterns*; 2017; 95−107.
(37) Wang, H.; He, P.; Li, N.; Cao, J. Pose Recognition of 3D Human Shapes via Multi-View CNN with Ordered View Feature Fusion. *Electronics* **2020**, *9*, 1368.
(38) Zhao, R.; Pang, M.; Wang, J. Classifying airborne LiDAR point clouds via deep features learned by a multi-scale convolutional neural network. *Int. J. Geogr. Inf. Sci.* **2018**, *32*, 960−979.
(39) Zhou, Y.; Tuzel, O. Voxelnet: End-to-end learning for point cloud based 3d object detection. *2018 IEEE/CVF Conference on Computer Vision and Pattern Recognition*; 2018; pp 4490−4499.
(40) Wu, Z.; Song, S.; Khosla, A.; Yu, F.; Zhang, L.; Tang, X.; Xiao, J. 3D ShapeNets: A deep representation for volumetric shapes. *2015 IEEE Conference on Computer Vision and Pattern Recognition (CVPR)*; 2015; pp 1912−1920.
(41) Graham, B.; Engelcke, M.; van der Maaten, L. 3D Semantic segmentation with submanifold sparse convolutional networks. *2018 IEEE/CVF Conference on Computer Vision and Pattern Recognition*; 2018; pp 9224−9232.
(42) Qi, C. R.; Su, H.; Mo, K. PointNet: Deep Learning on Point Sets for 3D Classification and Segmentation. *2017 IEEE Conference on Computer Vision and Pattern Recognition (CVPR)*; 2017; pp 652−660.
(43) Khazari, A. E.; Que, Y.; Sung, T. L.; Lee, H. J. Deep Global Features for Point Cloud Alignment. *Sensors* **2020**, *20*, 4032.
(44) Wu, B.; Liu, Y.; Lang, B.; Huang, L. DGCNN: Disordered graph convolutional neural network based on the gaussian mixture model. *Neurocomputing* **2018**, *321*, 346−356.
(45) Qi, C. R.; Yi, L.; Su, H.; Guibas, L. J. Pointnet++: Deep hierarchical feature learning on point sets in a metric space. *NIPS'17: Proceedings of the 31st International Conference on Neural Information Processing Systems*; 2017; pp 5105−5114.
(46) Wang, Y.; Sun, Y.; Liu, Z.; Sarma, S. E.; Bronstein, M. M.; Solomon, J. M. Dynamic graph cnn for learning on point clouds. *ACM Trans. Graph.* **2019**, *38*, 1−12.
(47) Widyaningrum, E.; Bai, Q.; Fajari, M. K.; Lindenbergh, R. C. Airborne Laser Scanning Point Cloud Classification Using the DGCNN Deep Learning Method. *Remote Sens.* **2021**, *13*, 859.

https://doi.org/10.1021/acsomega.1c04393
ACS Omega 2021, 6, 31699−31715

(48) Xing, Z.; Zhao, S.; Guo, W.; Guo, X.; Wang, Y. Processing Laser Point Cloud in Fully Mechanized Mining Face Based on DGCNN. *ISPRS Int. J. Geo-Inf.* **2021**, *10*, 482.
(49) Lim, J.; Ryu, S.; Park, K.; Choe, Y. J.; Ham, J.; Kim, W. Y. Predicting Drug−Target Interaction Using a Novel Graph Neural Network with 3D Structure-Embedded Graph Representation. *J. Chem. Inf. Model.* **2019**, *59*, 3981−3988.
(50) Ye, S.; Liang, J.; Liu, R.; Zhu, X. Symmetrical Graph Neural Network for Quantum Chemistry with Dual Real and Momenta Space. *J. Phys. Chem. A* **2020**, *124*, 6945−6953.
(51) Torng, W.; Altman, R. B. Graph Convolutional Neural Networks for Predicting Drug-Target Interactions. *J. Chem. Inf. Model.* **2019**, *59*, 4131−4149.
(52) Kim, M.; Park, S.; Danielson, J.; Irwin, J.; Stensaas, G.; Stoker, J.; Nimetz, J. General External Uncertainty Models of Three-Plane Intersection Point for 3D Absolute Accuracy Assessment of Lidar Point Cloud. *Remote Sens.* **2019**, *11*, 2737.
(53) Schweidtmann, A. M.; Rittig, J. G.; König, A.; Grohe, M.; Mitsos, A.; Dahmen, M. Graph Neural Networks for Prediction of Fuel Ignition Quality. *Energy Fuels* **2020**, *34*, 11395−11407.
(54) Roszak, R.; Beker, W.; Molga, K.; Grzybowski, B. A. Rapid and Accurate Prediction of pKa Values of C−H Acids Using Graph Convolutional Neural Networks. *J. Am. Chem. Soc.* **2019**, *141*, 17142−17149.
(55) Korolev, V.; Mitrofanov, A.; Korotcov, A.; Tkachenko, V. Graph Convolutional Neural Networks as "General-Purpose" Property Predictors: The Universality and Limits of Applicability. *J. Chem. Inf. Model.* **2020**, *60*, 22−28.

https://doi.org/10.1021/acsomega.1c04393
ACS Omega 2021, 6, 31699−31715